Supporting information:

Observation of slow magnetic relaxation phenomena in spatially isolated π-radical ions

Shohei Koyama*, Kazunobu Sato, Masahiro Yamashita, Ryota Sakamoto, and Hiroaki Iguchi*

Table of Contents

Crystallographic data

Table S1. Crytallographic data of BTI-xy·Toluene

Radiation type, wave length	Mo Kα, 0.71073 Å
Empirical formula	$C_{43}H_{27}CoN_3O_6$
Formula weight	681.67 g/mol
Crystal system	Monoclinic
Space group	$P2_1/m$
Crystal size	0.2 × 0.08 × 0.08 mm^3
Crystal color	yellow
Crystal shape	Needle
Unit cell dimensions	a = 8.8004(4) Å
	b = 18.9270(6) Å
	c = 11.5824(4) Å
	β = 105.010(5) °
Temperature	300 K
Z	2
Density (calculated)	1.215 Mg/m^3
Absorption coefficient	0.082 mm^{-1}
R_1, $wR_2[I > 2\sigma(I)]$	0.0558, 0.1585
R_1, wR_2[all data]	0.0688, 0.1709
$F(000)$	708
Goodness of fit on F^2	1.032

Table S2. Crytallographic data of **$CoCp_2$BTI-xy** (**1**)

Radiation type, wave length	Mo Kα, 0.71073 Å
Empirical formula	$C_{46}H_{27}CoN_3O_6$
Formula weight	776.63 g/mol
Crystal system	Trigonal
Space group	*R*-3*c*
Crystal size	0.4 × 0.3 × 0.1 mm^3
Crystal color	Black
Crystal shape	Block
Unit cell dimensions	*a* = 13.8716(2) Å
	c = 33.7979(8) Å
Temperature	120 K
Z	6
Density (calculated)	1.374 Mg/m^3
Absorption coefficient	0.512 mm^{-1}
R_1, wR_2[$I > 2\sigma(I)$]	0.0557, 0.1662
R_1, wR_2[all data]	0.0607, 0.1712
F(000)	2394
Goodness of fit on F^2	1.069

Table S3. Crytallographic data of **CoCp*$_2$BTI-xy** (**2**)

Radiation type, wave length	Mo Kα, 0.71073 Å
Empirical formula	$C_{56}H_{57}CoN_3O_6$
Formula weight	926.97 g/mol
Crystal system	Monoclinic
Space group	*C*2/*c*
Crystal size	0.15 × 0.15 × 0.05 mm^3
Crystal color	Dark green
Crystal shape	Block
Unit cell dimensions	*a* = 19.8607(12) Å
	b = 18.4970(7)
	c = 12.9906(6) Å
	β =102.711(5) °
Temperature	120 K
Z	4
Density (calculated)	1.323 Mg/m^3
Absorption coefficient	0.425 mm^{-1}
R_1, $wR_2[I > 2\sigma(I)]$	0.0760, 0.1875
R_1, wR_2[all data]	0.1058, 0.2108
F(000)	1956
Goodness of fit on F^2	1.063

Cyclic Voltammogram

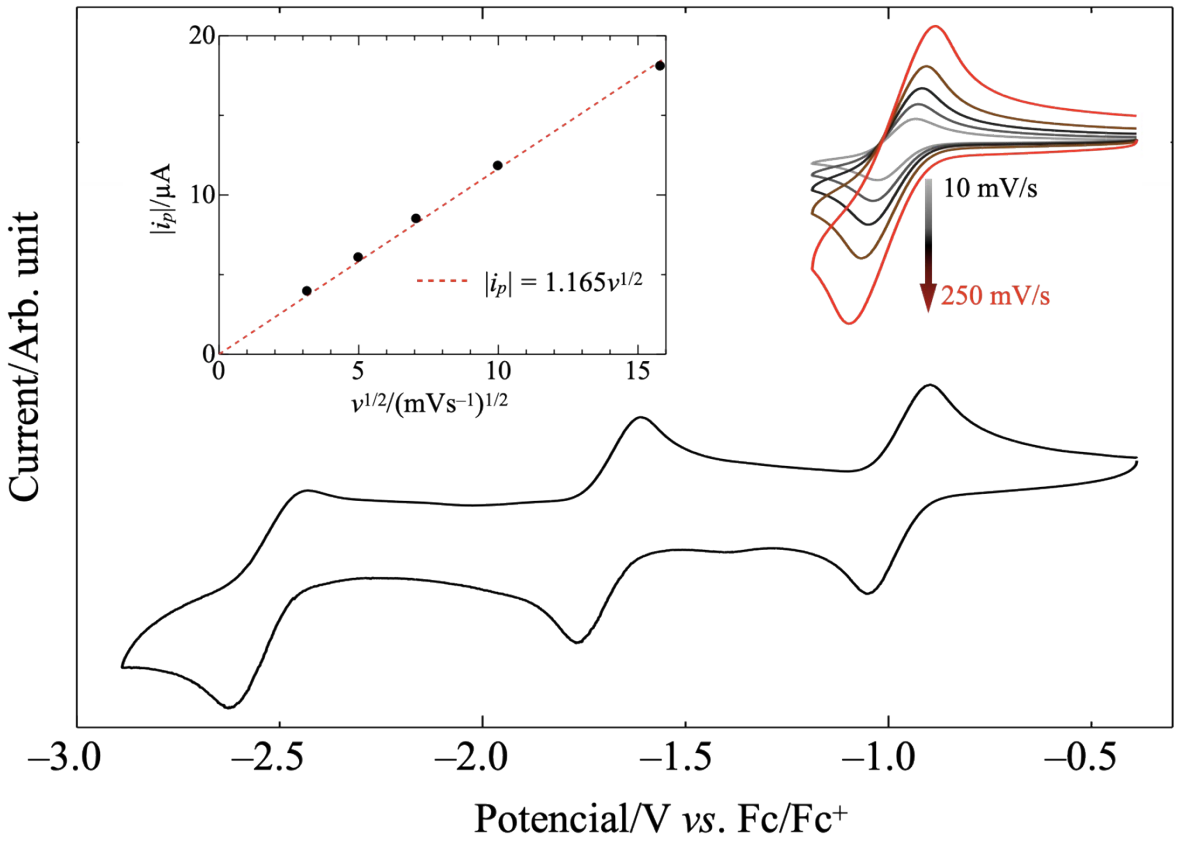

Figure S1. Cyclic voltammogram of BTI-xy. (Upper) The first reduction waves are shown for sweeps at 10, 25, 50, 100, and 250 mV/s. Inset shows the peak current plotted against 1/2 power of the sweep rates. (Bottom) The cyclic voltammogram at 100 mV/s.

Spin density of BTI-xy radical

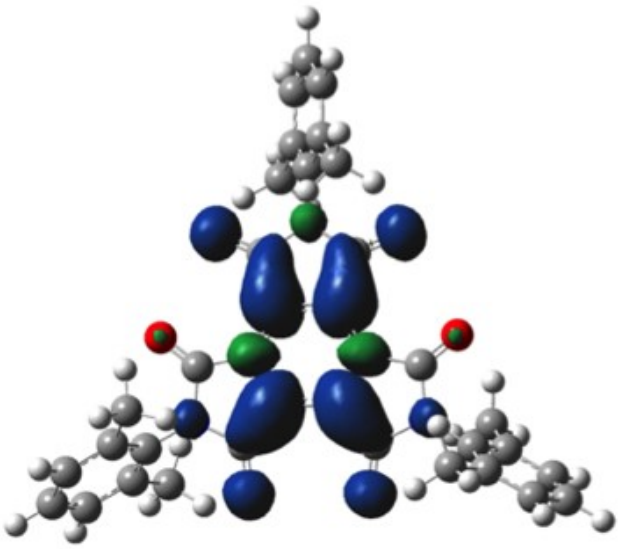

Figure S2. Spin density of BTI-xy radical calculated by DFT with optimized structure. Isosurface value:0.0004.

ESR spectra at –130 °C

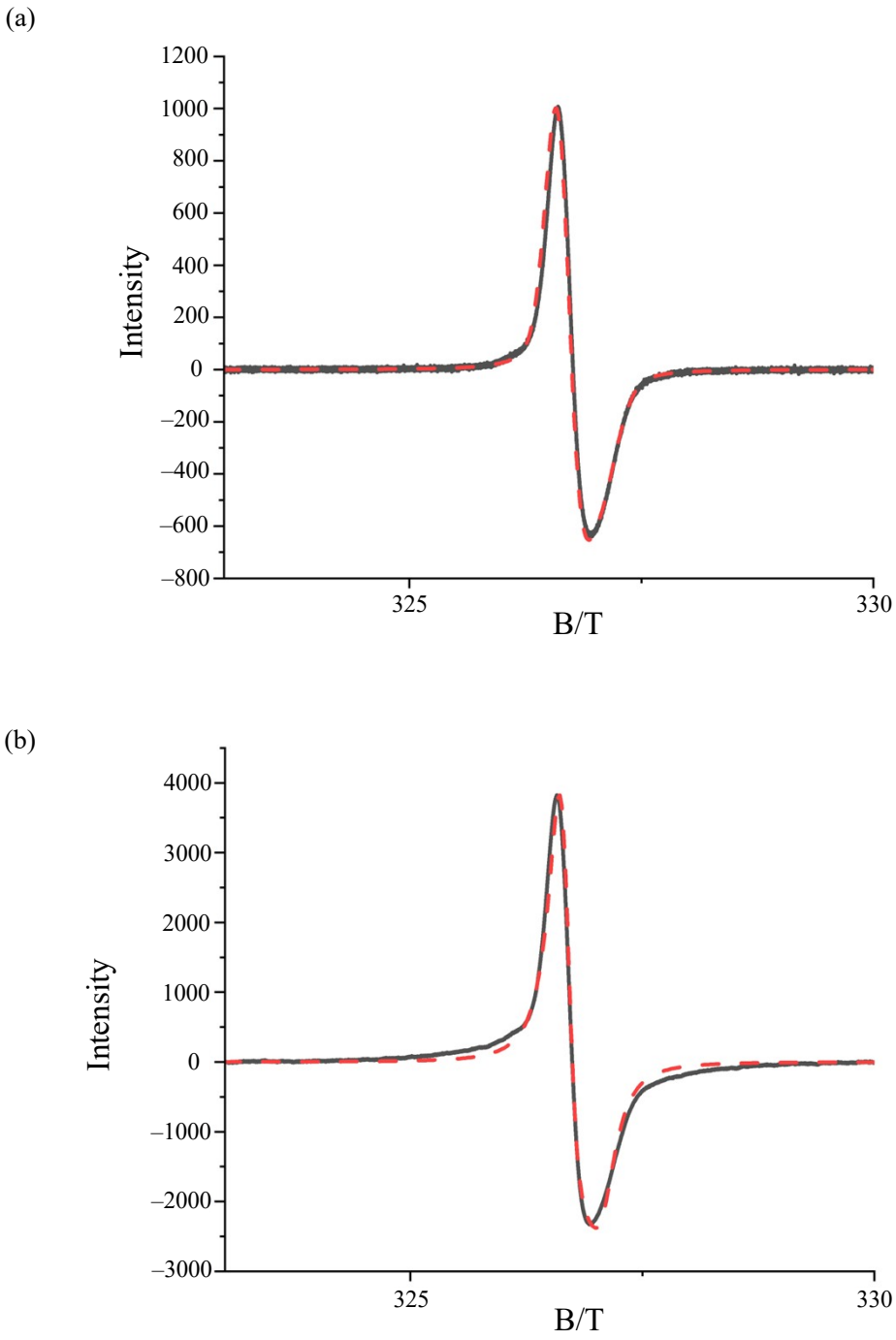

Figure S3. ESR spectra of **1** (a) and **2** (b) diluted in 0.2 mM DMF:benzene solution at –130 °C.

Table S4. Fitting parameter of the ESR spectra of **1** (a) and **2** (b) diluted in 0.2 mM DMF:benzene solution.

	1(RT)	**1**(–130°C)	**2**(RT)	**2**(–130°C)
Frequency/GHz	9.1626	9.1626	9.1614	9.1626
Nuclear spin	0	0	0	0
Electron spin	0.5	0.5	0.5	0.5
g_{perp}	2.0044	2.0040	2.0037	2.0040
g_{para}	2.0017	2.0014	2.0022	2.0016
σ_{perp}/mT	0.28	0.27	0.19	0.20
σ_{para}/mT	0.35	0.35	0.20	0.24
Lorentz ratio/%	50	50	100	100
Gauss ratio/%	50	50	0	0

Input file used for fitting of $\chi_M T$ plot

By utilizing the input file below, we have performed fitting to estimate the interaction between spins. For the form of the spin Hamiltonian, please refer to the PHI software User manual, available at http://www.molmag.manchester.ac.uk/software/phi_manual.pdf (accessed January 2023).

```
****ion
Ee
****fit
simplex
2.00
gf 1 4
----
-1
zJ
----
****mag
Tmag 1.85
****sus
bsus 0.1
****params
opmode fit s
****end
```

$\chi_M T$ vs. T plot

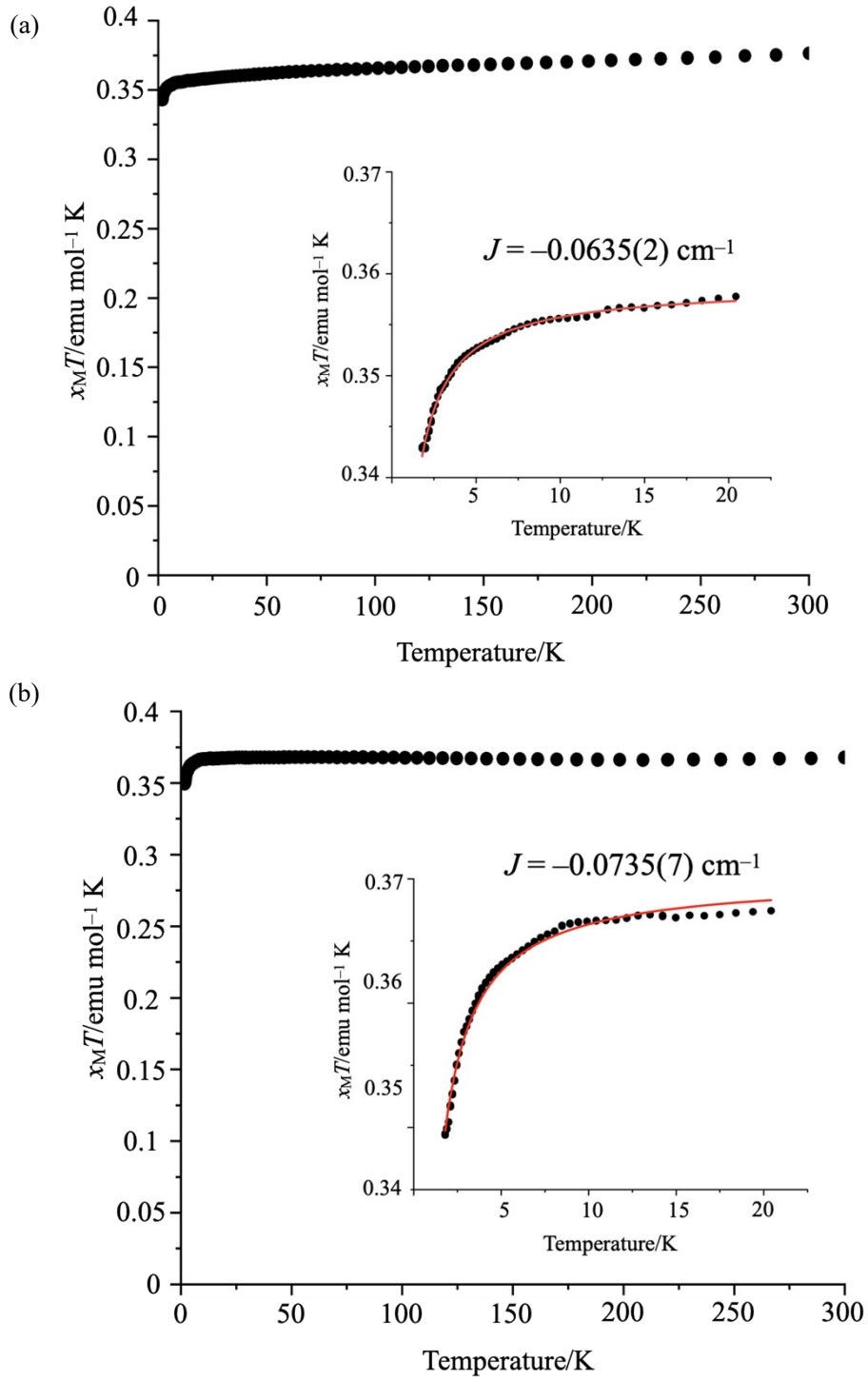

Figure S4. $\chi_M T$ vs. T plot of **1** (a) and **2** (b). Inset shows the data focused on the temperature below 10 K.

Field-dependent *ac* susceptibility of 1@2 K

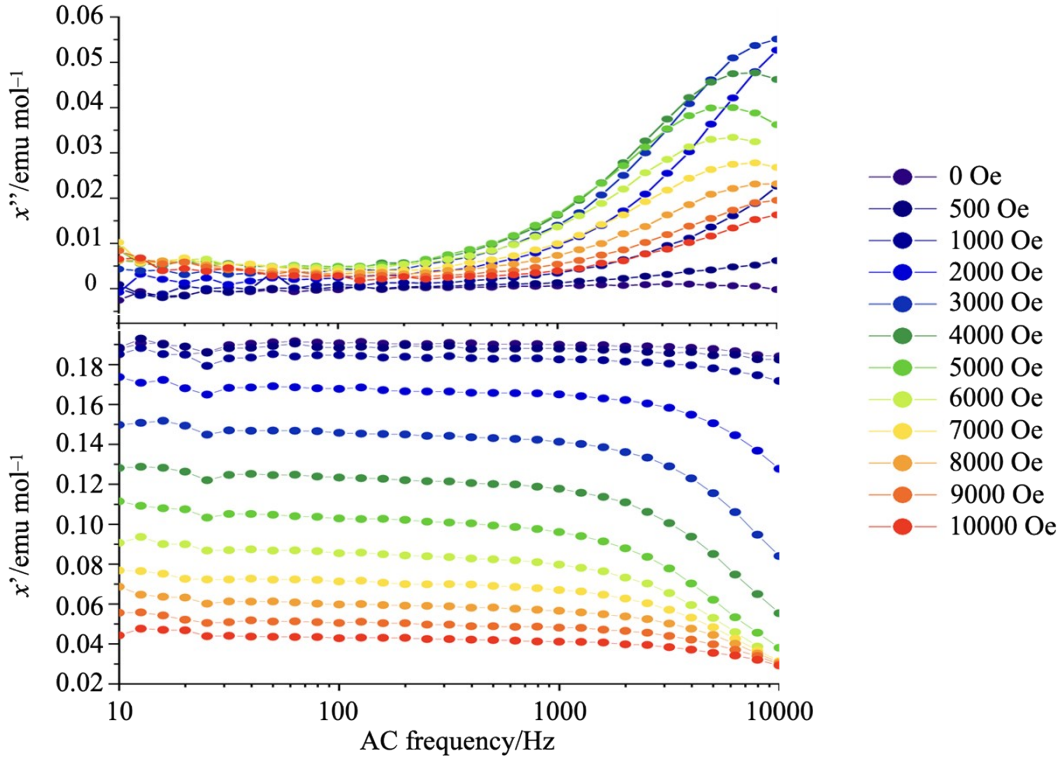

Figure S5. Field-dependent *ac* susceptibility for **1** at 2 K. The solid line connecting the colored dots are the guide for eye.

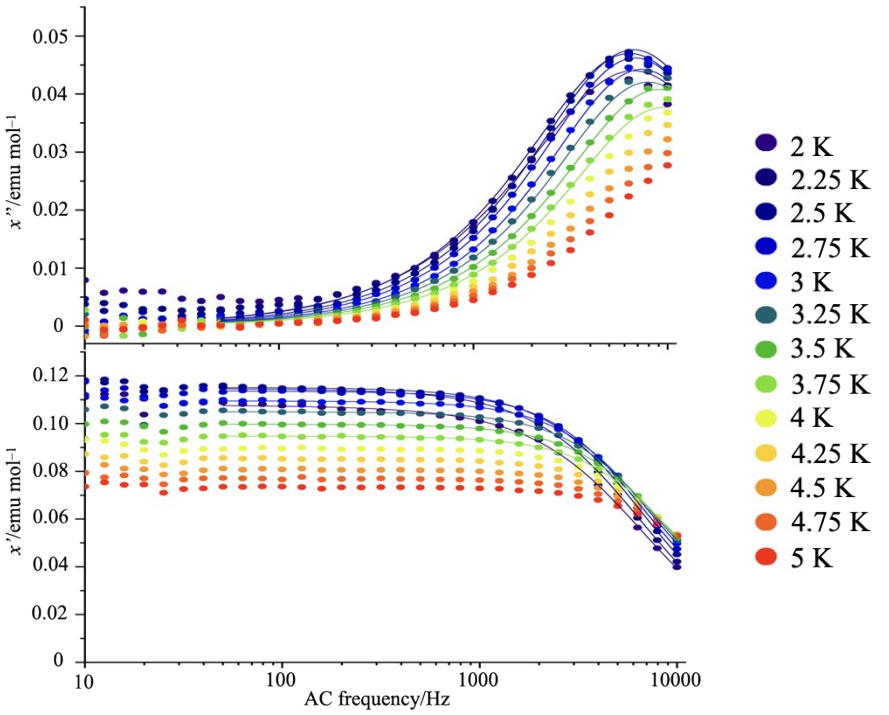

(a)

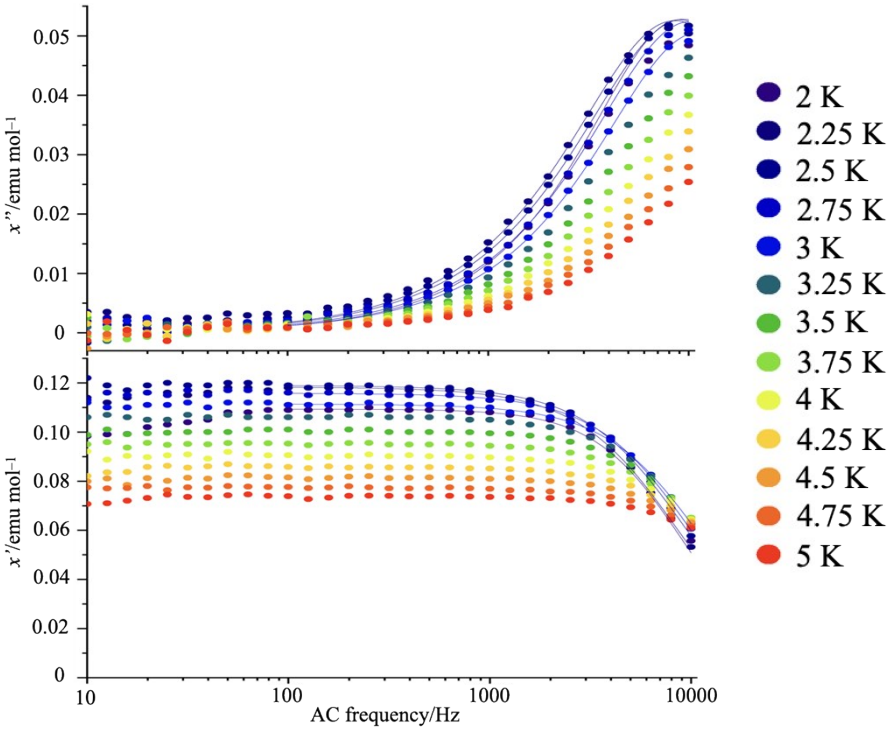

Temperature-dependent *ac* susceptibility of 1@0.5 T

(b)

Figure S6. Temperature-dependent *ac* susceptibility for crystalline (a), and ground (b) samples of **1** under an applied static magnetic field of 0.5 T.

Field-dependent *ac* susceptibility of 2@5 K, 7.5 K, 10 K

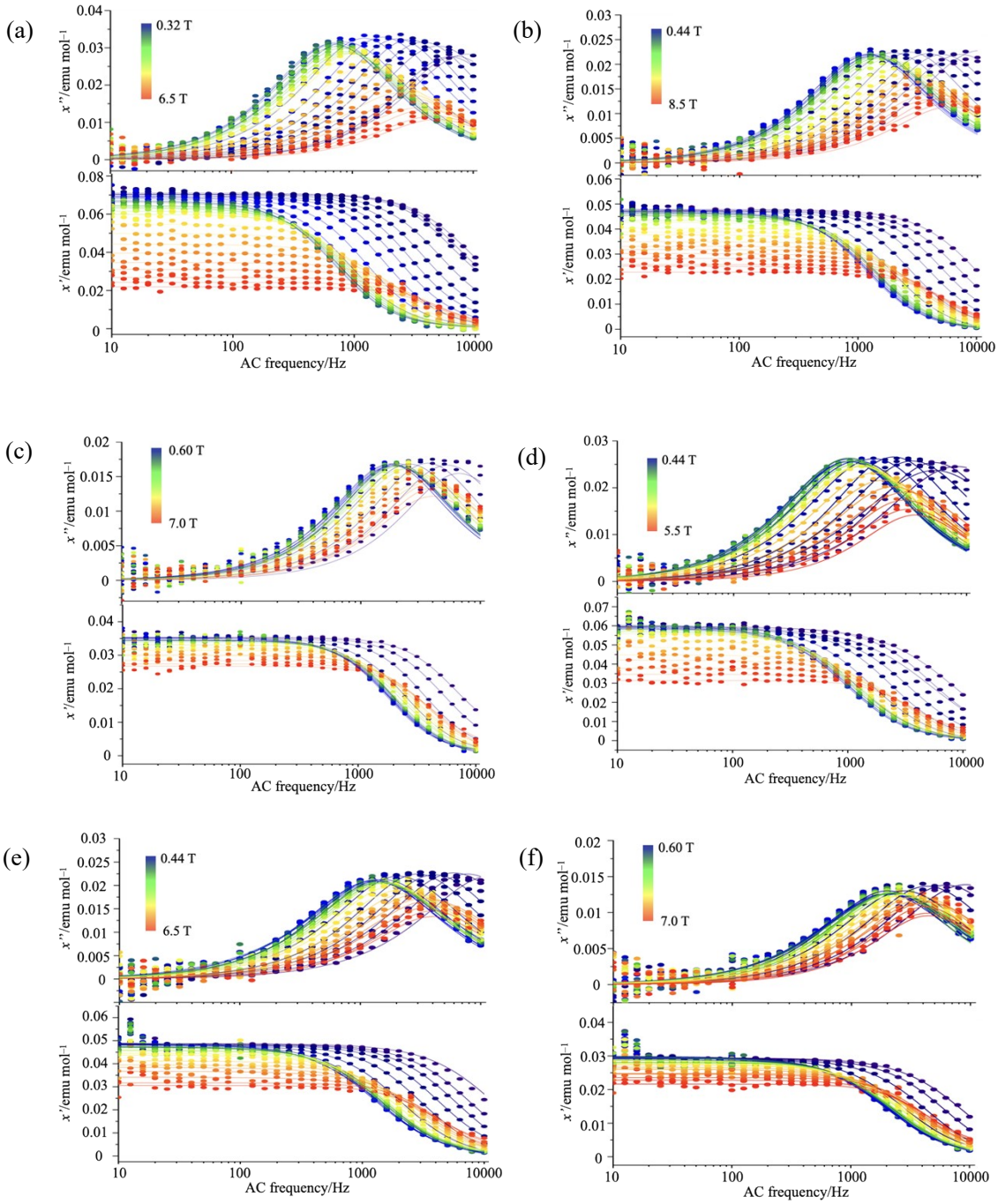

Figure S7. Field-dependent *ac* susceptibility for **2** at 5 K (a), 7.5 K (b), 10 K (c) and for the ground sample of **2** at 5 K (d), 7.5 K (e), 10 K (f). The solid lines are the fitting line by Cole-Cole plot.

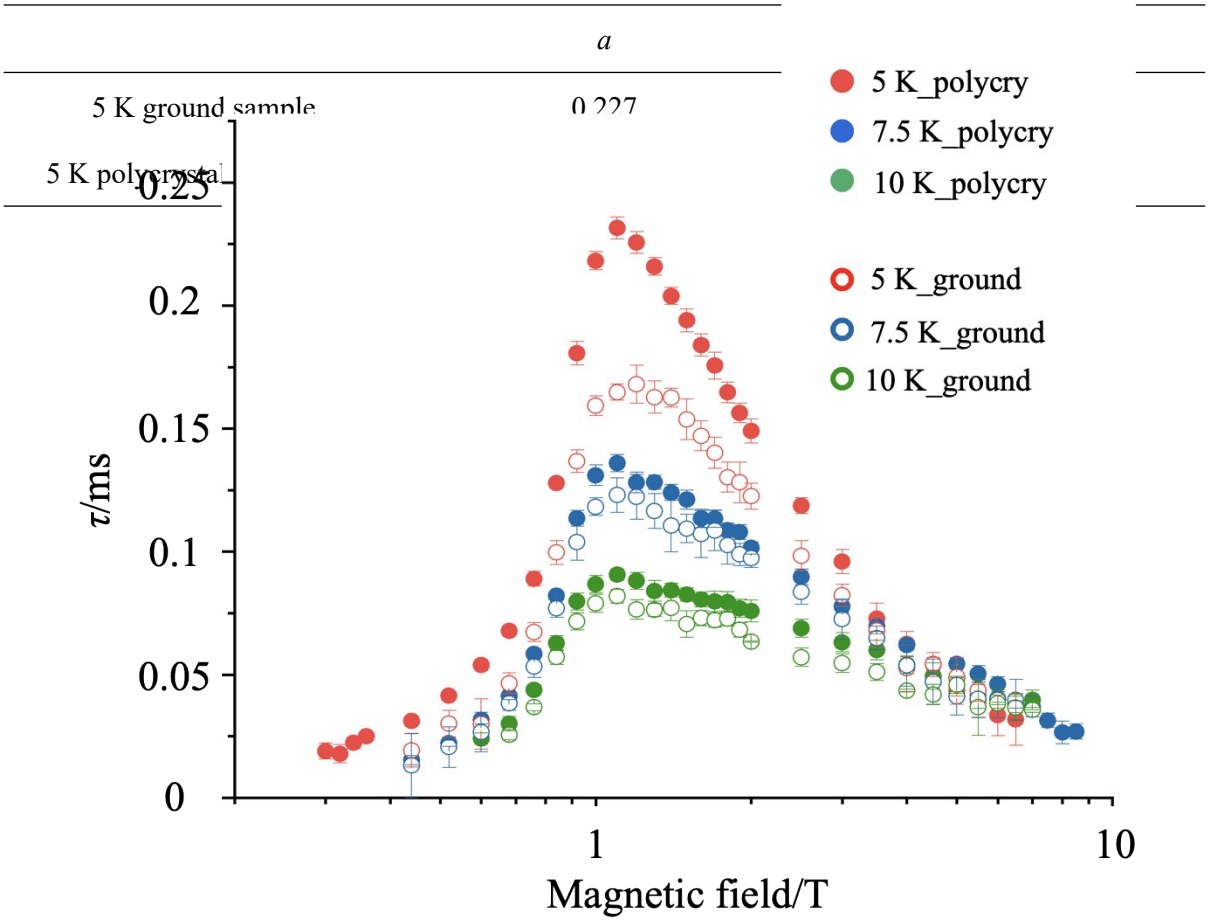

Field-dependent relaxation time of 2@5 K, 7.5 K, 10 K

Figure S8. Magnetic field dependence of τ extracted from ac susceptibility at 5.0 K (red), 7.5 K (blue), 10 K (green) for polycrystalline **2** (filled circle) and ground **2** (hollow circle).

7.5 K ground sample	0.155	–0.722
7.5 K polycrystalline sample	0.168	–0.745
10 K ground sample	0.0885	–0.481
10 K polycrystalline sample	0.102	–0.471

Table S5. Fitting parameters for the magnetic field dependence of τ in **2** at the high magnetic field region fitted by $\tau = aB^n$

(a)

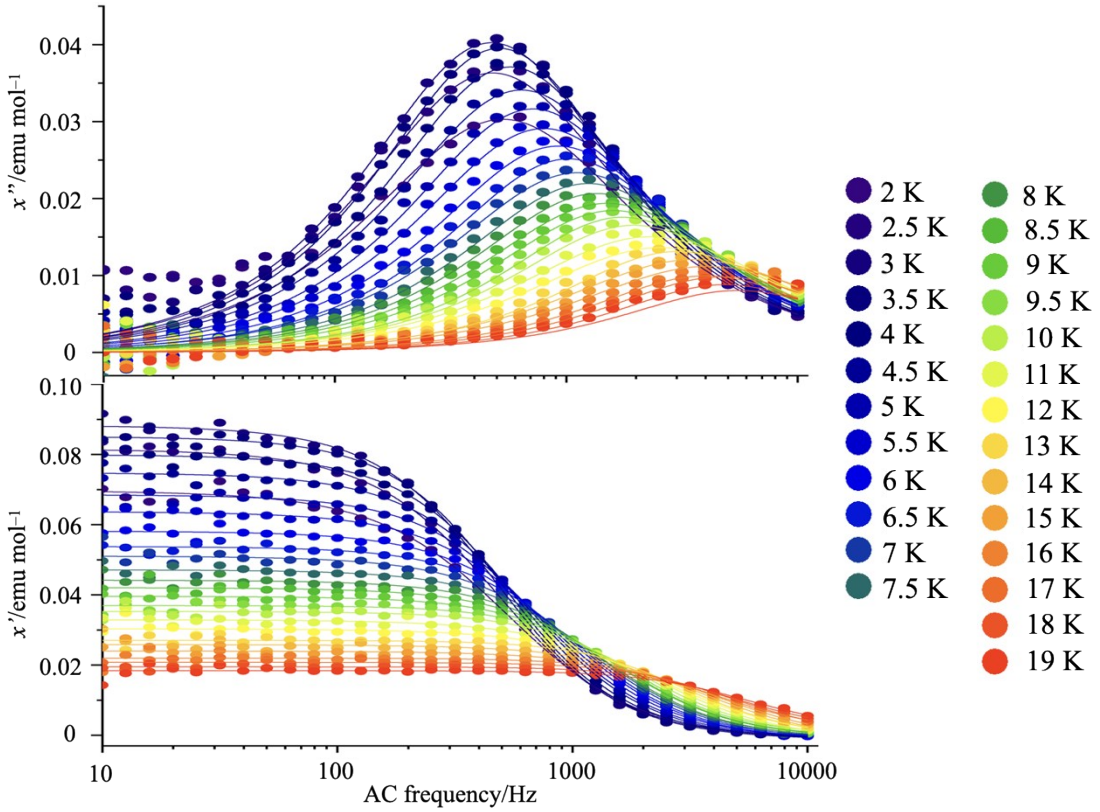

(b)

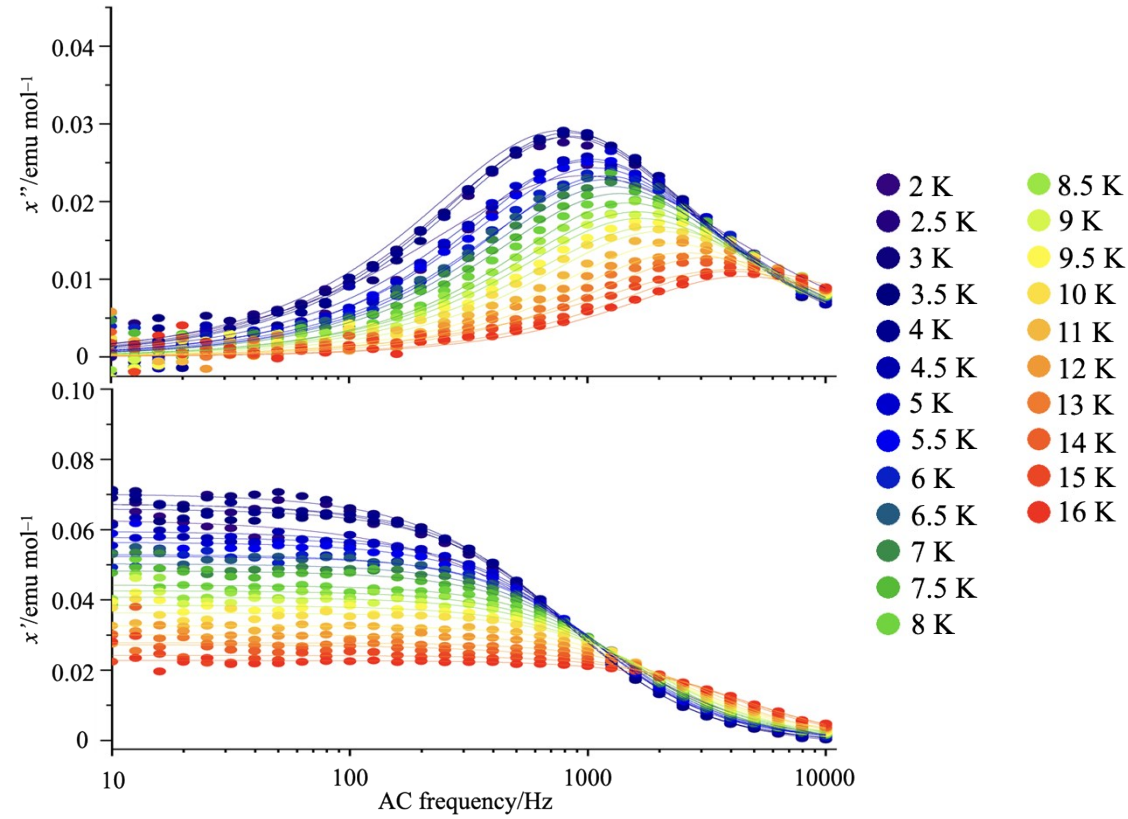

Temperature-dependent *ac* susceptibility of 2@1 T

Figure S9. Temperature-dependent *ac* susceptibility for crystalline (a) and ground (b) samples of **2** under an applied static magnetic field of 1 T. The solid lines are the fitting line by Cole-Cole plot.

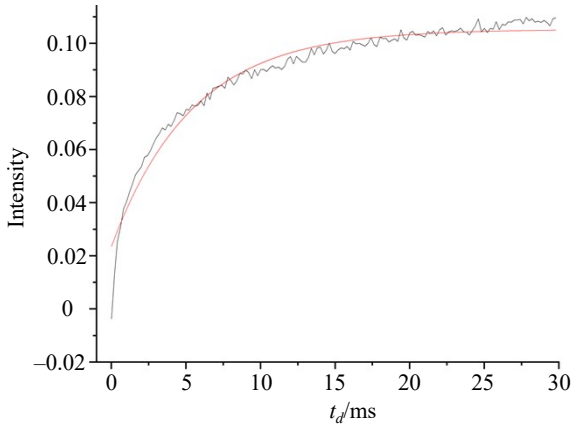

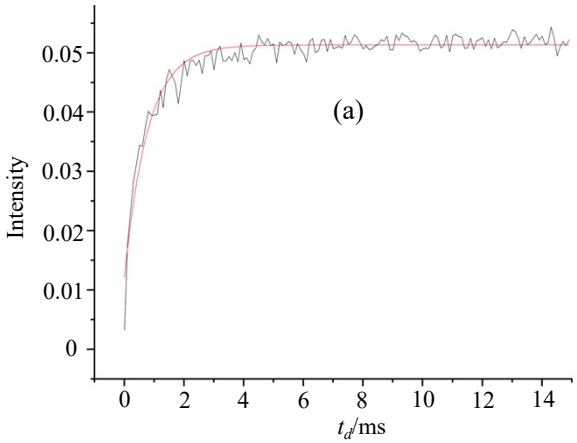

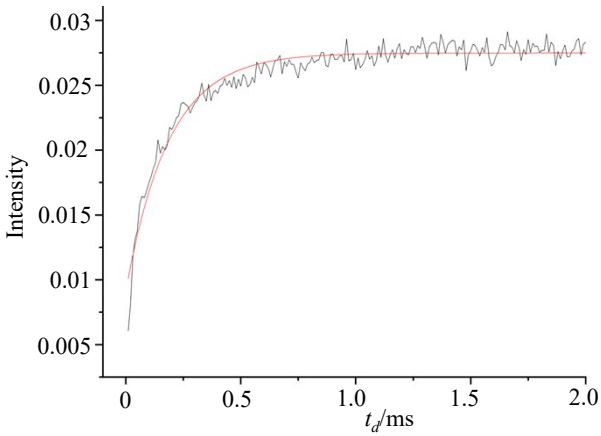

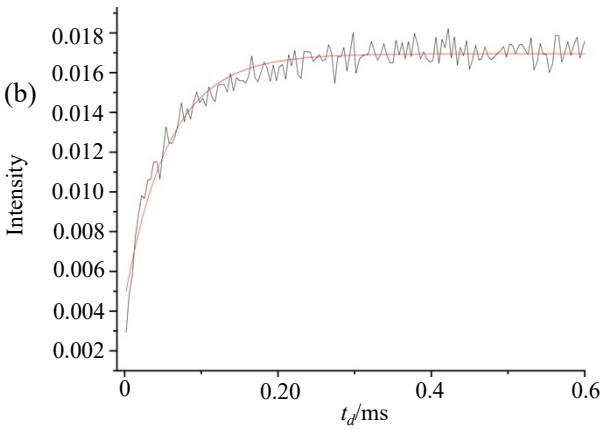

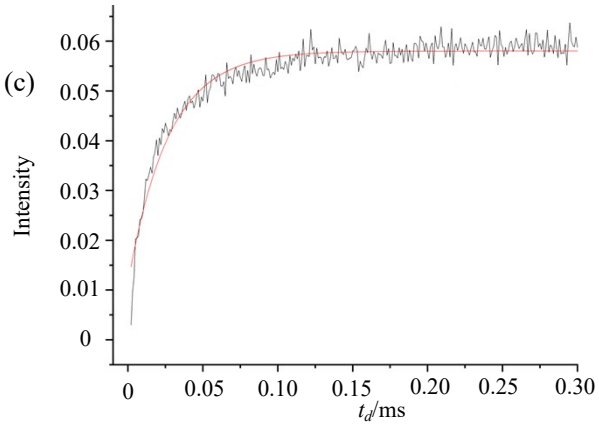

The intensity of three pulse echoes in 1

(d) (e)

Figure S10. Changes in echo intensities for **1** with respect to t_d at 10 K (a), 20 K (b), 30 K (c), 40 K (d) and 50 K (e). Red lines are the fitting line shown in experimental section.

Table S6. Parameters of the fitting line shown in experimental section for **1**.

		10 K	20 K	30 K	40 K	50 K
1	I_0	0.10525	0.05131	0.02748	0.01694	0.05801
	I	–0.08188	–0.03968	–0.01834	–0.0124	–0.04669
	T_1	5.39553	0.78013	0.18701	0.05738	0.02702

		10 K	20 K	30 K	40 K	50 K

2	I_0	0.14915	0.07311	0.03591	0.14605	0.08885
	I				–0.12697	–0.07056
	T_1	5.41			0.04937	0.0271

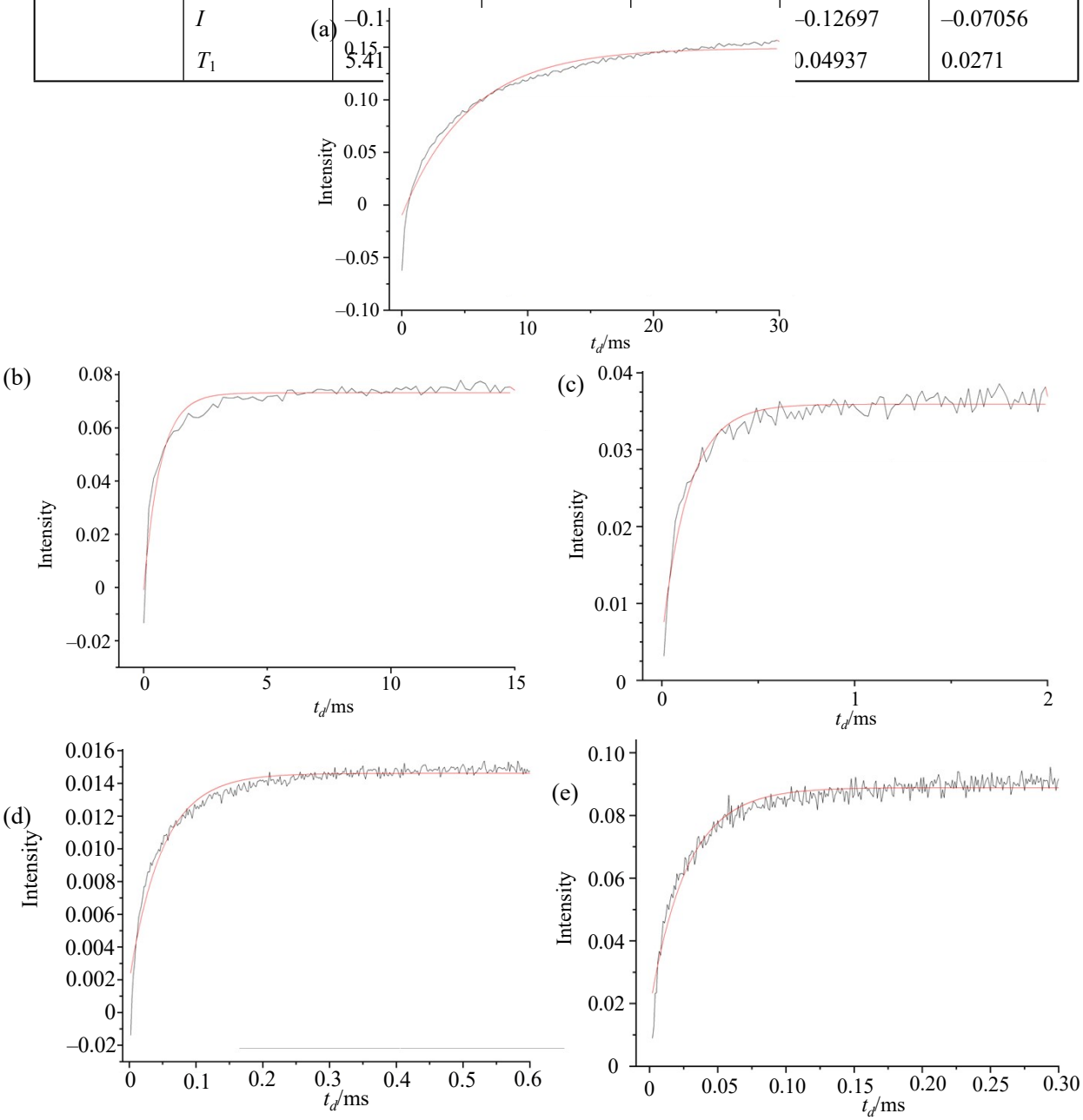

The intensity of three pulse echo in 2

Figure S11. Changes in echo intensities for **2** with respect to t_d at 10 K (a), 20 K (b), 30 K (c), 40 K (d) and 50 K (e). Red lines are the fitting line shown in experimental section.

Table S7. Parameters of the fitting line shown in experimental section for **2**.

The intensity of two pulse echo

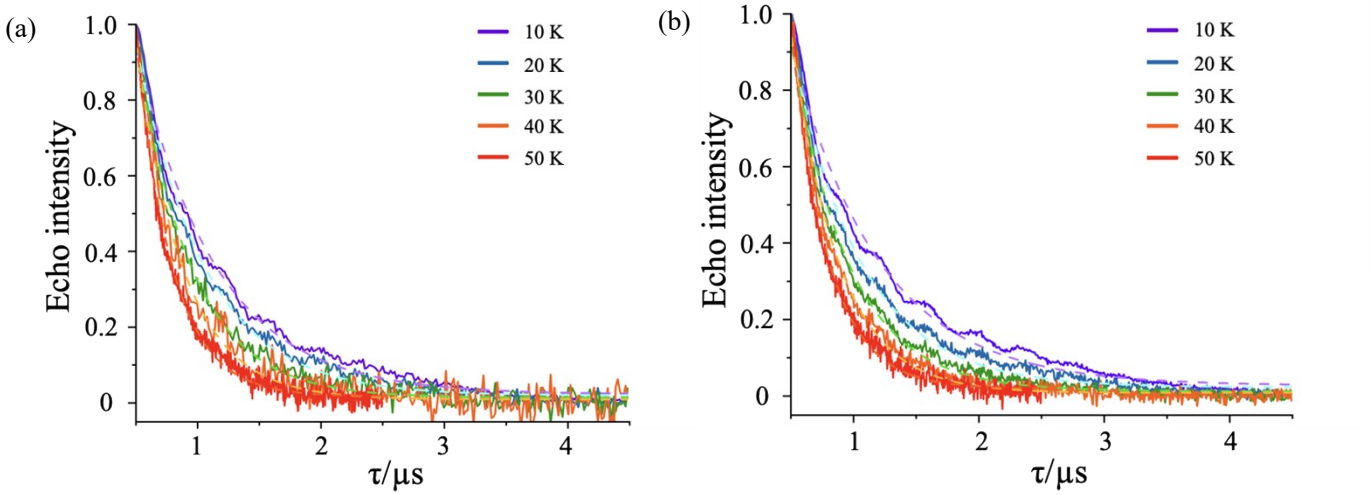

Figure S12. Changes in two pulse echo intensities for **1** (a) and **2** (b) with respect to τ. Broken lines present the fitting line with the following parameters listed in Table S8.

		10 K	20 K	30 K	40 K	50 K
1	I_0	0.02261	0.01917	0.01371	0.00941	0.01702
	I	1.98906	2.29075	2.81319	3.46705	5.23863
	T_2	1.29673	1.11011	0.90603	0.76644	0.58417
2	I_0	0.02704	0.02257	0.01247	0.0084	0.01935
	I	1.81177	2.21836	2.72355	3.62226	5.20648
	T_2	1.40532	1.10995	0.91697	0.74739	0.58633

Table S8. Fitting parameters of the changes in two pulse echo intensities.

Solid-state Raman and absorption spectroscopy

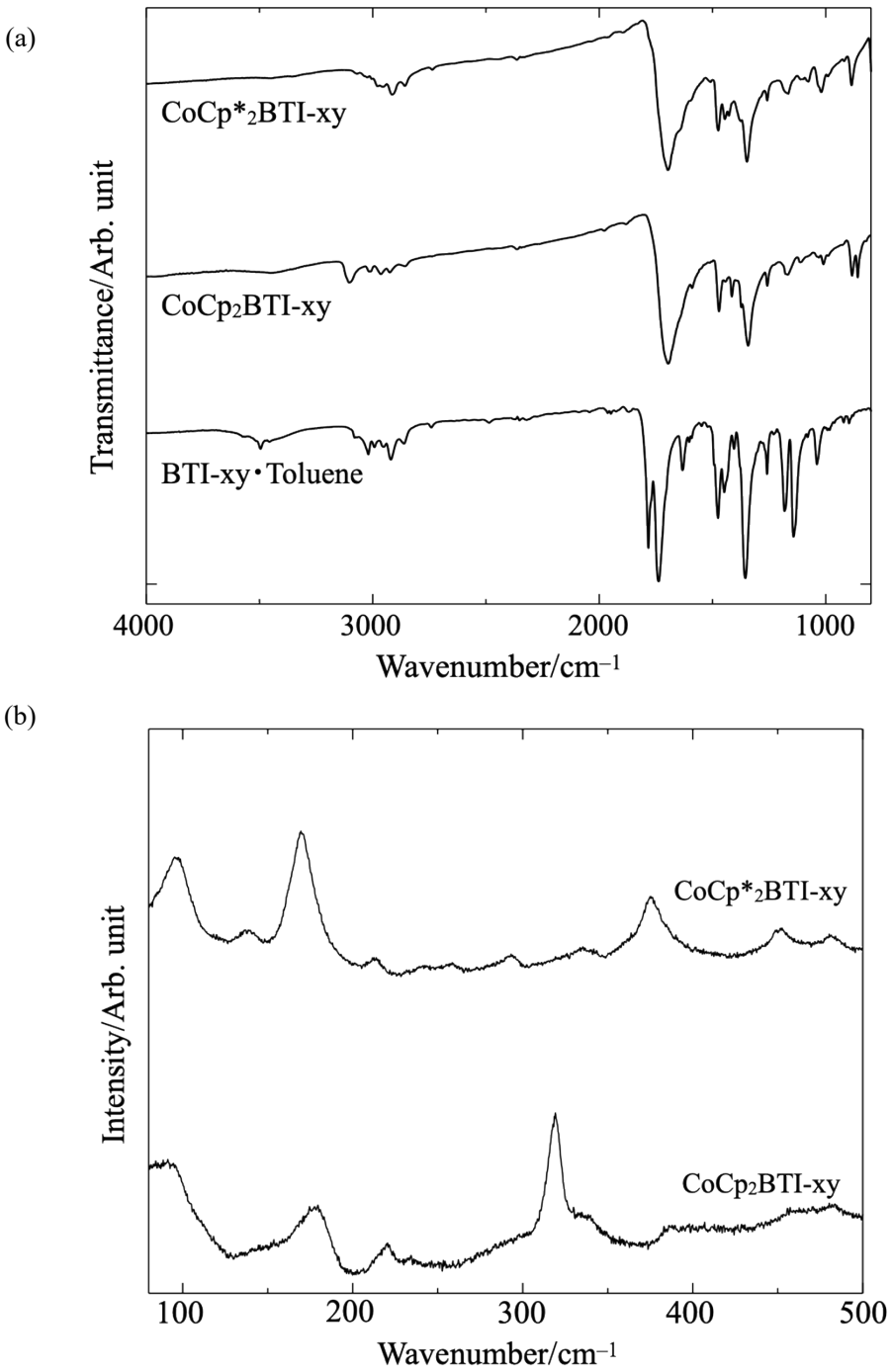

Figure S13. IR absorption spectra (a) and Raman spectra (b) of the obtained compounds.